INTERNATIONAL JOURNAL OF SCIENTIFIC RESEARCH AND INNOVATIVE STUDIES
ISSN: 2820-7157
www.ijsrisjournal.com

February 2025 **Volume 5** **Number 1** **23-30**

Received Date: December 20, 2025 **Accepted Date: January 12, 2026** **Published Date: February 01, 2026**

Impulse responses of a floating cylinder for recovering wave energy

Imad EL BYDARY

Engineering Mechanics and Innovation Laboratory, Hassan II University, Casablanca, Morocco

Abstract:

Over the last few decades, the world has focused its attention on renewable energies and how to exploit them in the right way. Recovering wave energy and converting it into electrical energy is of major interest to researchers. This work focuses on calculating the impulse response of a floating cylinder subjected to wave action using two methods. One is analytical, based on the article by Cummins, and the other is numerical, using the "NEMOH" code, in order to compare the two methods.

Keywords: Energy recovery, Waves, Impulse response, Floating cylinder, "NEMOH" code, Morison model.

Introduction:

Renewable energies are now an essential for moving away from petroleum and its derivatives. Wave energy is considered a type of renewable marine energy.

To exploit wave energy in the best way possible and convert it into electrical energy, a floating energy converter is required. This converter can take several forms and be positioned in various locations within the sea, depending on the desired energy recovery.

The problem of wave energy recovery involves several factors that need to be studied, in particular the impulse response of the floating body, which summarizes its interaction with the waves in the time domain. Knowledge of this response will be extremely useful, particularly in studying the movement of the body and subsequently optimizing control of its oscillatory movement.

For years, the calculation of impulse response has remained stuck in the analytical realm, even in theories without any serious scientific output, in order to move towards the numerical aspect and compare the two aspects. ***Cummins*** **[1]** provided two new representations of the equations of motion of an oscillating ship, taking into account the six degrees of freedom in order to calculate the impulse response in each representation. It should be noted that the representations are fairly general and apply to both transient and periodic motions. ***Oglivie [2]*** continued Cummins' work by applying the Fourier transform to the differential equation of motion, and also established the relationships between the frequency and time domains. ***J. Falnes [3]*** emphasized the non-causality of two impulse response functions of a floating body. ***A. Jabrali [4]*** studied the motion of an oscillating cylinder under the action of waves, comparing the results obtained using the NEMOH code and the semi-analytical method. ***EV. Ermanyuk [5]*** used the impulse response as a means of evaluating the added mass and damping coefficient of a circular cylinder floating in a fluid.

The objective of our work is to study the impulse response of a cylinder floating vertically and being "pounded" using two calculation methods, one based on the equation of motion of

the cylinder and the other based on the numerical method using the NEMOH calculation code provided by the openWEC application **[6]**.

1. Description of the problem

We consider a floating cylinder with density ρ, radius R and length L in a pounding motion (single degree of freedom) and subjected to a sinusoidal Airy wave.

Table 1: Dimensions of the system under study.

Diameter D(m)	2.62
Length L(m)	13
Swell amplitude A_m (m)	0.5
Swell period T(s)	2

The study is conducted in a non-Galilean reference frame$R(O,\vec{x},\vec{y},\vec{z})$ with O as the origin of the reference frame placed on the swell at any point. This study is limited to the pounding motion of the disc. The only degree of freedom in the problem is the variable denoted here as "y(t)".

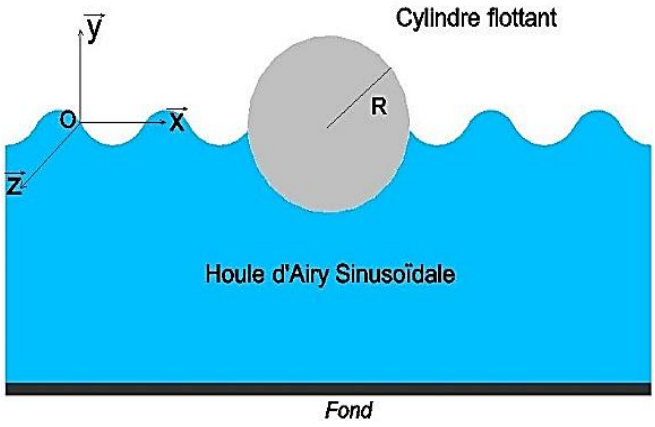

Figure 1: Diagram of the floating cylinder.

2. Numerical approach

2.1. Calculation of the Impulsive Response by NEMOH

The basic tool used in this study is the impulse response function.

In 1964, ***Ogilvie [2]*** continued the work of ***Cummins [1]*** by applying the Fourier transform. He established the relationships between the frequency and time models by establishing the following relationships:

$$A(\omega,\breve{U}) = A_\infty(\breve{U}) - \frac{1}{\omega}\int_0^\infty K(t,\widetilde{U})\,sin(\omega t)\,dt \qquad (1)$$

$$B(\omega,\breve{U}) = B_\infty(\breve{U}) - \frac{1}{\omega}\int_0^\infty K(t,\widetilde{U})\,cos(\omega t)\,dt \qquad (2)$$

Where$A(\omega,\breve{U})$ s the added mass matrix,$B(\omega,\widehat{U})$ represents the damping matrix,$\widehat{U}$ the average velocity of the floating body,ω pulsation, and$K(t,\widetilde{U})$ impulse response function.

And by inverse Fourier transform, the impulse response is given by:

$$K(t,\breve{U}) = \frac{2}{\pi}\int_0^\infty \left(A(\omega,\breve{U}) - A_\infty(\breve{U})\right) sin(\omega t)\,d\omega \qquad (3)$$

$$K(t,\breve{U}) = \frac{2}{\pi}\int_0^\infty \left(B(\omega,\breve{U}) - B_\infty(\breve{U})\right) cos(\omega t)\,d\omega \qquad (4)$$

Where: $A_\infty(\breve{U}) = \lim_{\omega\to\infty} A(\omega,\breve{U})$
$B_\infty(\breve{U}) = \lim_{\omega\to\infty} B(\omega,\breve{U})$

Before calculating the impulse response function, we must calculate the hydrodynamic coefficients in the frequency domain (added mass, radiation damping) using the OpenWEC application **[6]** based on the NEMOH calculation code.

The NEMOH code allows us to insert the geometric data of the cylinder and information about the swell, and obtain the movement of the cylinder and the speed and hydrodynamic coefficients, added mass$A(\omega)$,A_∞ , and hydrodynamic damping$B(\omega)$,B_∞ .

The impulse response is calculated using Maple software, making both integral expressions (3) and (4) numerically calculable.

3. Analytical Approach

3.1. Calculation of the Impulse Response using the Morison Model

We consider two-dimensional flow in the plane$(\vec{x},\vec{y})$ around a disc floating on the free surface of the fluid.

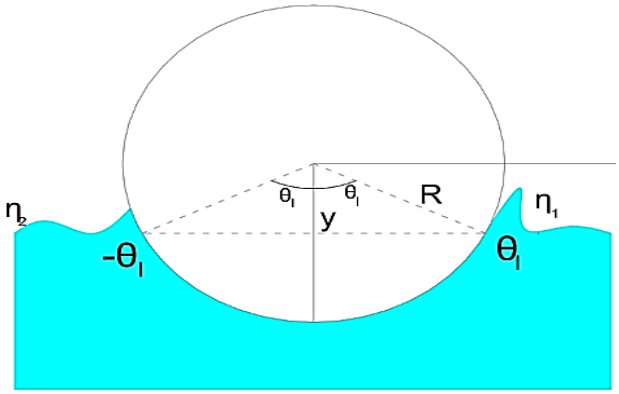

Figure 2: 2D diagram of the floating cylinder.

The fundamental principle of dynamics applied to a solid body of mass$m$ for a translational motion with a single degree of freedom is written as:

$$m\ddot{y}\vec{y} = \vec{P} + \vec{F}_a + \vec{F}_m \qquad (5)$$

Where$\vec{P} = m\vec{g}$ is the force of gravity,$\vec{F}_m$ is the Morison force representing the inertial and viscous forces exerted by the fluid ($\vec{F}_m = \underbrace{\rho_e C_m V\, \ddot{y}\vec{y}}_{\vec{F}_I} + \underbrace{\frac{1}{2}\rho_e C_d S\dot{y}|\dot{y}|\vec{y}}_{\vec{F}_D}$) where$\dot{y}$ and$\ddot{y}$ are respectively the velocity and acceleration of the cylinder relative to the fluid,ρ_e is the density of the fluid,C_d is the drag coefficient,C_m is an inertia coefficient, $V = \pi R^2 L$ is the volume of the cylinder,$S = 2RL\arccos(\frac{y}{R})$ is the submerged surface area of the cylinder, and$\vec{F}_a$ is the buoyant force, which is defined by:

$$F_a = -\rho_e gLRy\left[\sin\left(\theta_l + \frac{\eta_1}{R}\right) + \sin\left(\theta_l + \frac{\eta_2}{R}\right)\right] + \rho_e gLR^2\left(\theta_l + \frac{\eta_1+\eta_2}{2R} + \frac{1}{4}\left(\sin\left(2\left(\theta_l + \frac{\eta_1}{R}\right)\right) + \sin\left(2\left(\theta_l + \frac{\eta_2}{R}\right)\right)\right)\right) \qquad (6)$$

Where$\theta_l = \arccos(\frac{y}{R})$,L is the length of the cylinder,g is the acceleration due to gravity,R is the radius of the cylinder.
The equation for the free surface is written as:

$$\eta_1 = \mathrm{a}\sin\left(\omega t - k(x - R\sin\theta_l)\right) \qquad (7)$$

$$\eta_2 = \mathrm{a}\sin\left(\omega t - k(x + R\sin\theta_l)\right) \qquad (8)$$

Substituting these expressions into equation (5) gives:

$$(m + \rho_e C_m V)\ddot{y} + \frac{1}{2}\rho_e C_d S V_m \dot{y} = F\cos(\omega t) - mg - \rho_e gLRy\left[\sin\left(\theta_l + \frac{\eta_1}{R}\right) + \sin\left(\theta_l + \frac{\eta_2}{R}\right)\right] + \rho_e gLR^2\left[\theta_l + \frac{\eta_1+\eta_2}{2R} + \frac{1}{4}\left(\sin 2\left(\theta_l + \frac{\eta_1}{R}\right) + \sin 2\left(\theta_l + \frac{\eta_2}{R}\right)\right)\right] \qquad (9)$$

Where: V_m is the average velocity.

We linearize this equation by performing an expansion in the vicinity of the equilibrium positiony_e .

Let us assume that the wavelength of the swell is greater than the radius of the cylinder, i.e.$\lambda \gg R$, and that the amplitude of the swell is much smaller than the radius of the cylinder, i.e.$A_m \ll R$. Therefore,$\frac{\eta_1}{R} \ll 1$ and$\frac{\eta_2}{R} \ll 1$.

$$(m + \rho_e C_m V)\ddot{y} + \frac{\pi}{2}\rho_e C_d RLV_m\dot{y} - \rho_e gR^2 L\left[\arccos\left(\frac{y}{R}\right) - \frac{y}{R}\sqrt{1 - \left(\frac{y}{R}\right)^2}\right] = -mg + F\cos(\omega t) \qquad (10)$$

We introduce a Taylor expansion of order 1 in the vicinity of a position$Y$, such that:$Y = \frac{y - y_e}{R}$.

$$(m + \rho_e C_m V)\ddot{Y} + \frac{\pi}{2}\rho_e C_d RLV_m\dot{Y} + 2\rho_e RgL\sqrt{1 - \left(\frac{y_e}{R}\right)^2}\,Y = \frac{F\cos(\omega t)}{R} \qquad (11)$$

We set: $\boldsymbol{a} = (m + \rho_e C_m V)$, $\boldsymbol{b} = \frac{\pi}{2}\rho_e C_d RLV_m$,

$$\boldsymbol{c} = 2\rho_e RgL\sqrt{1 - \left(\frac{y_e}{R}\right)^2}\,, \quad \boldsymbol{e} = \frac{F}{R}\,.$$

Equation (11) becomes:

$$a\ddot{Y} + b\dot{Y} + cY = e\cos(\omega t) \qquad (12)$$

After solving equation (12) using Maple software, the expression of y(t) includes a particular solution and another homogeneous solution. For the rest of this paper, we will work only with the particular solution that corresponds to the established part.

And by identification with ***Cummins'*** equation **[1]**$y_i(t) = F_i[(K_{ii}^s)^2 + (K_{ii}^c)^2]^{\frac{1}{2}}\cos(\omega t)$, we obtain$\boldsymbol{K_{ii}^s}$,$\boldsymbol{K_{ii}^c}$.

The particular solution is therefore of the form:

$$\frac{y_i(t)}{F_i} = \frac{\sqrt{(-a\omega^2 + c)^2 + b^2\omega^2}}{a^2\omega^2 - 2ac\omega^2 + b^2\omega^2 + c^2}\cos\left(\omega t - \arctan\left(\frac{b\omega}{-a\omega^2 + c}\right)\right) \qquad (13)$$

Then, by identification, we have:

$$K_{ii}^c = \frac{-a\omega^2 + c}{a^2\omega^2 - 2ac\omega^2 + b^2\omega^2 + c^2} \qquad (14)$$

$$K_{ii}^{s} = \frac{b\omega}{a^2\omega^2 - 2ac\omega^2 + b^2\omega^2 + c^2} \qquad (15)$$

Where K_{ii}^{c} and K_{ii}^{s} are the harmonic responses (these are the sine and cosine coefficients in the solution corresponding to an exciting force in cos (ω t)).

The impulse response function is related to these functions by:

$$K_{ii}(\tau) = \frac{2}{\pi}\int_0^{\infty} K_{ii}^{c}(\omega)\cos(\omega\tau)\ d\omega \qquad (16)$$

$$K_{ii}(\tau) = \frac{2}{\pi}\int_0^{\infty} K_{ii}^{s}(\omega)\sin(\omega\tau)\ d\omega \qquad (17)$$

Using Maple software, we can obtain an overview of the variation in the impulse response as a function of time.

4. Results and discussion

4.1. Numerical Method

The NEMOH code allows us to insert the geometric data of the cylinder and information about the waves, and obtain as results the movement of the cylinder and its speed, which are shown in Figures (3) and (4) respectively.

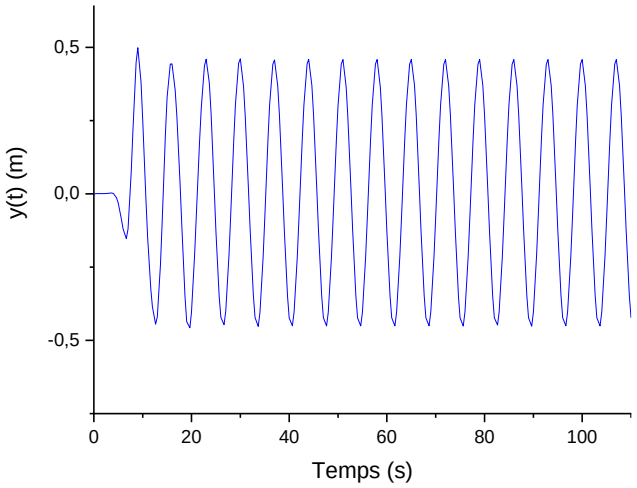

Figure 3: Pounding motiony(t) of the cylinder.

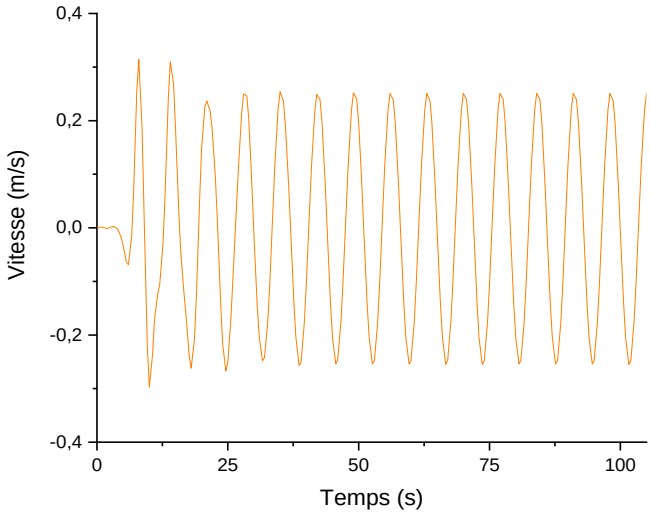

Figure 4: Speedv(t) as a function oft .

4.1.1. Added mass – Hydrodynamic damping hydrodynamic

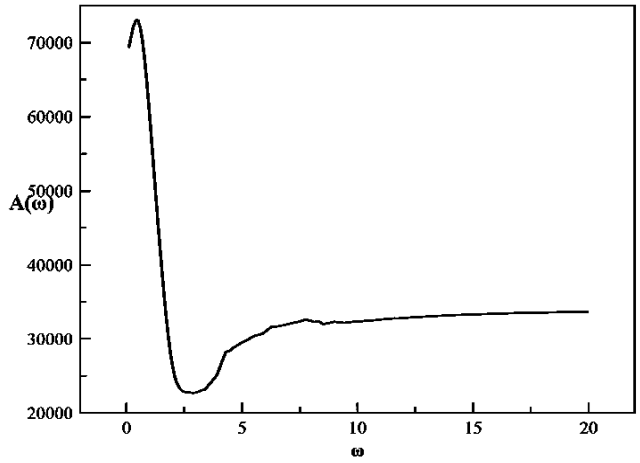

Figure 5: Added massA(ω) as a function ofω .

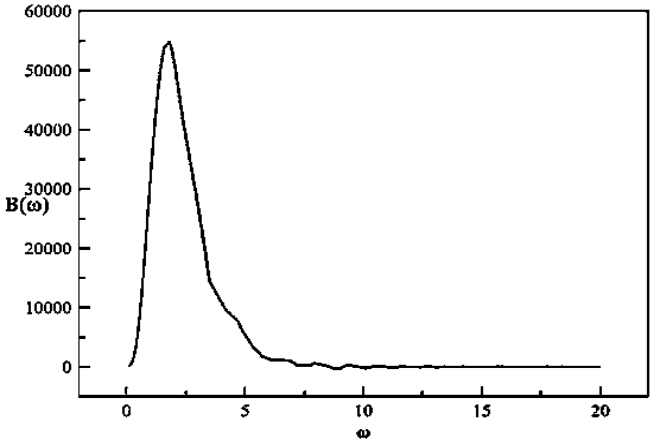

Figure 5: Hydrodynamic dampingB(ω) as a function ofω .

4.1.2. Impulse responses $K_a(t)$ and $K_b(t)$.

Based on the results found for the impulse response, we can see that the peak in the first few seconds (Figure 6, Figure 7) is due to the shock and also the memory effect resulting from the events closest to the shock.

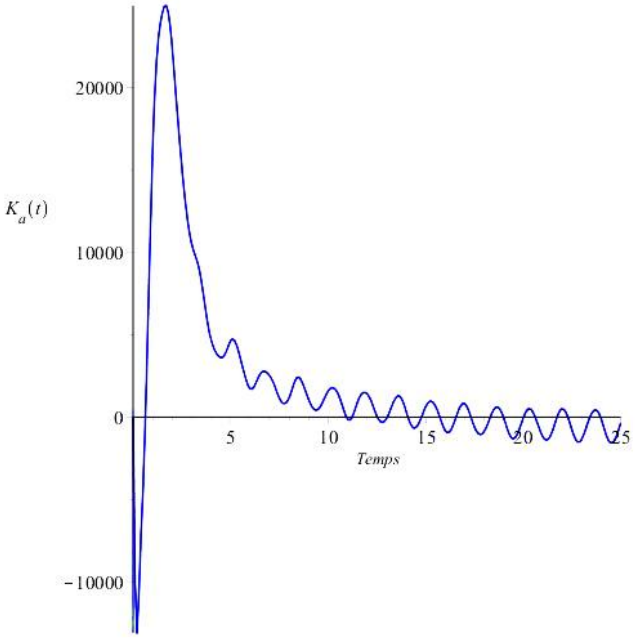

Figure 6: Impulse response function $K_a(t)$.

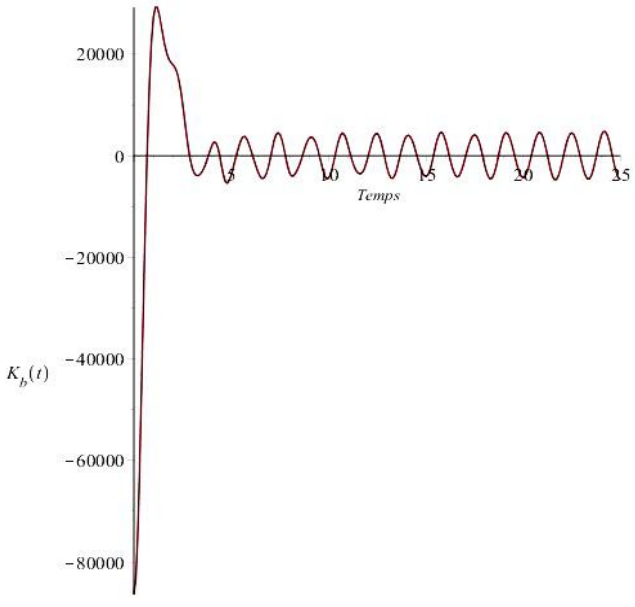

Figure 7: Impulse response function $K_b(t)$.

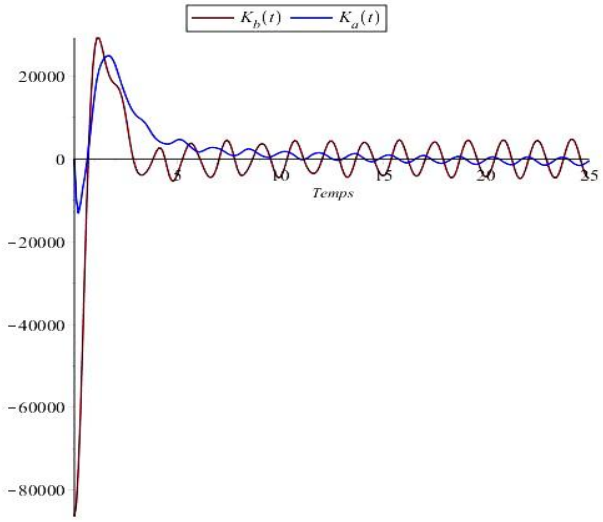

Figure 8: Comparison between the impulse response $K_a(t)$ and $K_b(t)$.

4.1.3. Effect of the cylinder radius

Table 2: Dimensions of the system studied.

Length L(m)	13
Swell amplitude A_m (m)	0.5

From Figure (9) and Figure (10), we can see that the radius has a significant effect when it takes on large values on damping, and the added mass, on the contrary, has no effect on the added mass when it has small values.

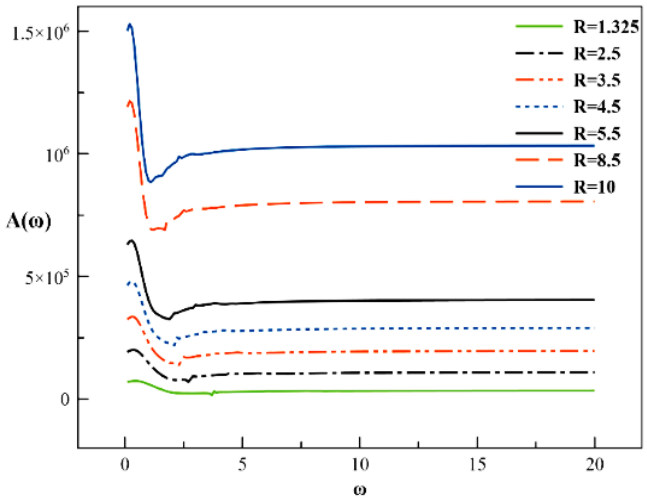

Figure 9: Added mass $A(\omega)$ as a function of ω .

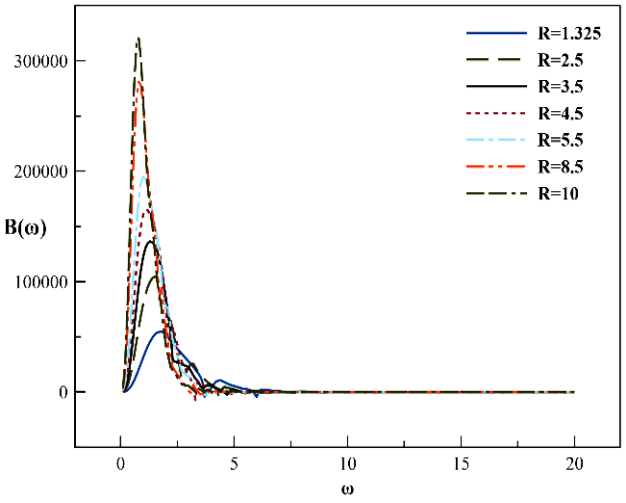

Figure 10: Hydrodynamic dampingB(ω) as a function ofω .

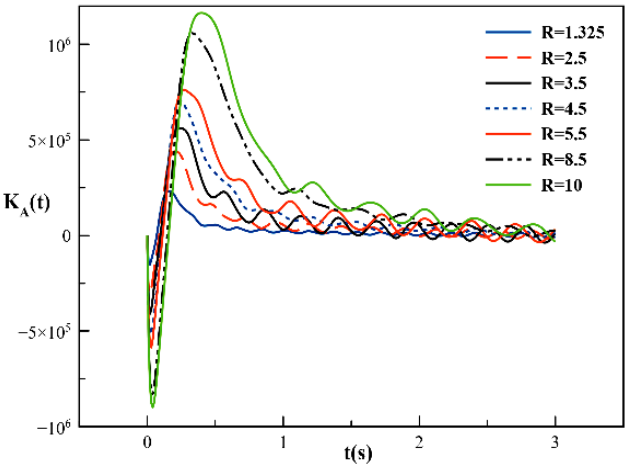

Figure 11: Impulse response function$K_a(t)$.

4.1.4. Effect of cylinder length

Table 3: Dimensions of the system studied.

Radius R (m)	2.5
Swell amplitude A_m (m)	0.5

From Figure (12) and Figure (13), we can see that the small length has no effect on the added mass and hydrodynamic damping because the cylinder does not have large dimensions.

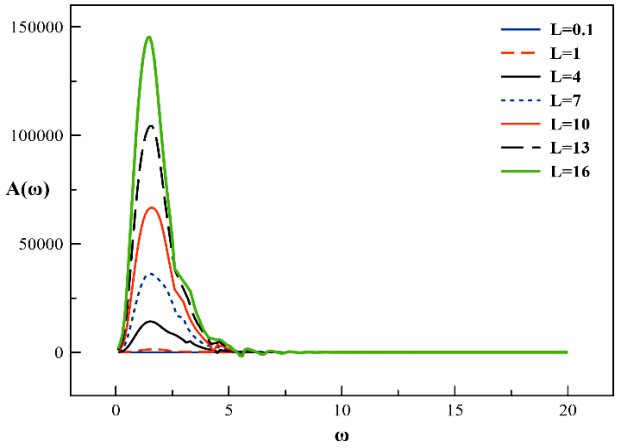

Figure 12: Added massA(ω) as a function ofω .

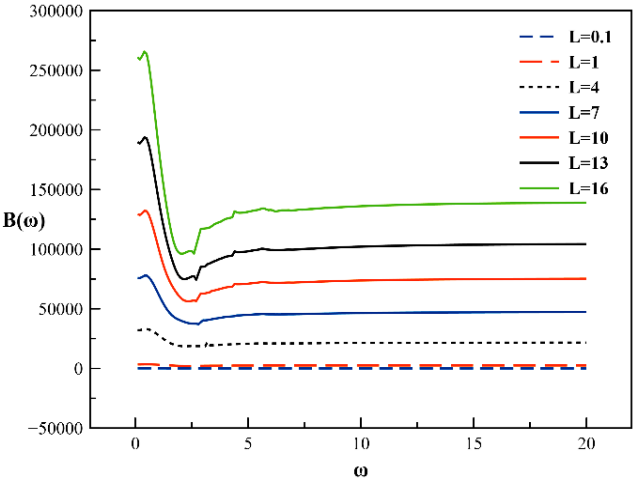

Figure 13: Hydrodynamic dampingB(ω) as a function ofω .

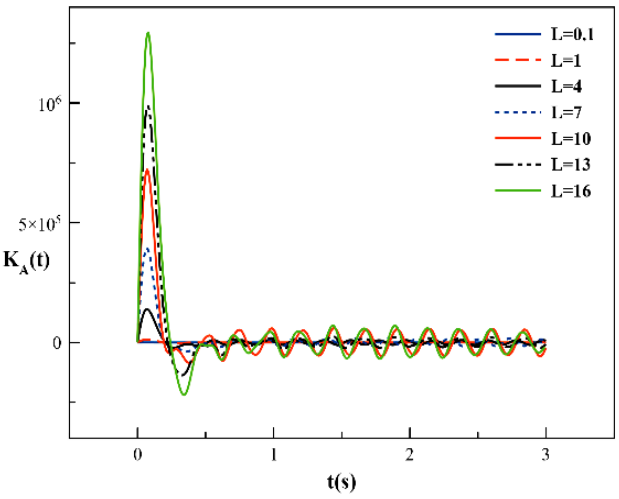

Figure 14: Impulse response function$K_a(t)$.

4.2. Analytical method

4.2.1. Case $V_m = 1.3\ m.s^{-1}$

Figure (15) shows the variation of the impulse response function as a function of time, in the case where the average velocity $V_m = 1.3\ m.s^{-1}$. This figure shows that the variation of $K_{ii}(t)$ remains almost sinusoidal; it is necessary to consider long times to observe damping.

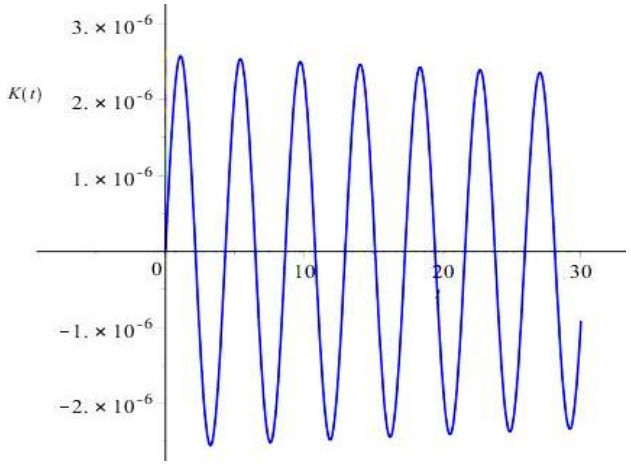

Figure 15: Impulse response function $K_{ii}(t)$ in the case where $V_m = 1.3\ m.s^{-1}$.

4.2.2. Case $V_m = 30\ m.s^{-1}$

Figure (16) shows the evolution of the impulse response function as a function of time, in the case where the average velocity is $V_m = 30\ m.s^{-1}$. According to this figure, we can see that the response $K_{ii}(t)$ dampens. From $t = 60\ s$ onwards, we will only have weak responses.

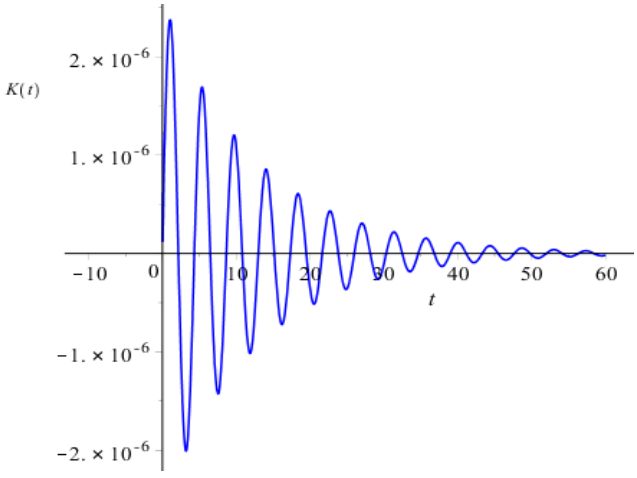

Figure 16: Impulse response function $K_{ii}(t)$ in the case where $V_m = 30\ m.s^{-1}$.

4.2.3. Case $V_m = 100\ m.s^{-1}$

Figure (17) shows the evolution of the impulse response as a function of time in the case where $V_m = 100\ m.s^{-1}$. We can see that the response $K_{ii}(t)$ weakens more quickly than in the last two cases.

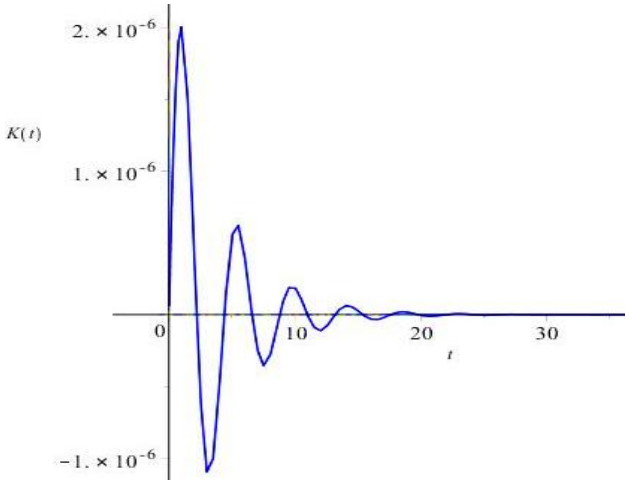

Figure 17: Impulse response function $K_{ii}(t)$ in the case where $V_m = 100\ m.s^{-1}$.

According to Figures (15), (16) and (17), we see that the higher the average velocity, the faster the $K_{ii}(t)$ weakens. This is due to the drag term in the Morison force, which contains the average velocity, i.e. the average velocity and the drag term vary proportionally. For this reason, when the average velocity increases, the drag term also increases, which immediately affects the impulse response $K_{ii}(t)$, causing it to weaken more quickly.

Conclusion

In order to achieve a good design and performance evaluation of wave energy converters, knowledge of the impulse response is important and very useful for calculating the movement of objects under excitation.

At the numerical level, we concluded that the two expressions of the impulse response $K_a(t)$ and $K_b(t)$ gave us the same variation in the impulse response over time with a small difference while maintaining the shape of the variation. In addition, we note the considerable effect of the radius and length of the cylinder on the added mass and hydrodynamic damping and, subsequently, the impulse response. To minimize the error between the responses $K_a(t)\ and K_b(t)$, we could develop the numerical programme to obtain overlapping curves. In the analytical approach, the average wave speed played a crucial role in the variation of the impulse response,

especially with large values $of K_{ii}(t)$, which dampens quickly due to the drag term in Morison's force.

References

[1] W.E. Cummins, The impulse response function and ship motion, Symposium on Ship Theory at the Institut Für Schiffbau der Universität Hamburg, 25–27 January 1962.

[2] T.F. Ogilvie, Recent Progress toward the Understanding and Prediction of Ship Motions. In: Proceedings of the 5th Symposium on Naval Hydrodynamics, Washington DC, USA, 1964.

[3] Yu, Z., J. Falnes, 1995. State-space modelling of a vertical cylinder in heave. Applied Ocean Research 17, 265–275.

[4] A. Jabrali, R. Khatyr, and J. Khalid Naciri, "Study of the motion of an oscillating cylinder under the action of waves", 13th Mechanics Congress, 11–14 April 2017 (Meknes, Morocco).

[5] Ermanyuk, E. The use of impulse response functions for evaluation of added mass and damping coefficient of a circular cylinder oscillating in linearly stratified fluid. Experiments in Fluids 28, 152–159 (2000).

[6] *https://github.com/tverbrug/openWEC* , Accessed on 30 November 2016.